Science of the Total Environment 912 (2024) 169539

Contents lists available at ScienceDirect

Science of the Total Environment

journal homepage: www.elsevier.com/locate/scitotenv

Real-time karst groundwater monitoring and bacterial analysis as early warning strategies for drinking water supply contamination

Jaime Fernández-Ortega *, Juan Antonio Barberá, Bartolomé Andreo

Department of Geology and Centre of Hydrogeology, University of Malaga (CEHIUMA), 29071 Malaga, Spain

HIGHLIGHTS

- An approach for early detection of karst groundwater faecal contamination is presented.
- Continuous monitoring of climate and water parameters was coupled to bacterial analysis.
- Sediment source contribution to the karst springs was qualitatively assessed.
- Human activities were responsible for the faecal bacteria detected at drinking water sources.
- Site specific karst groundwater protection strategies are crucial to prevent public health issues.

GRAPHICAL ABSTRACT

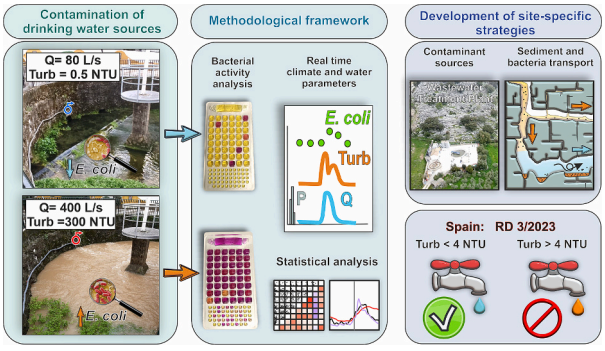

ARTICLE INFO

Editor: José Virgílio Cruz

Keywords:
Karst
Drinking water
Faecal contamination
Early-warning
Southern Spain

ABSTRACT

Karst aquifers have been globally exploited as a reliable source of drinking water but their intrinsic characteristics (concentrated recharge, high groundwater flow velocities, etc.) and the increase of anthropogenic pressures makes them highly vulnerable to pollution. Continuous monitoring of karst springs constitutes an effective approach for identifying episodic groundwater contamination and assuring safety conditions in drinking water supply systems. This study aims to improve groundwater protection insights through an integrated methodological approach based on real-time measurements of continuous water parameters coupled to bacterial analysis for the characterization of contamination events in a carbonate karst aquifer of a mountainous and rural area in S Spain. For this purpose, environmental, hydrodynamic and physico-chemical data in addition to bacterial activity (*Escherichia coli*) analysis were gathered from the analysis of eight flooding events at the two main outlets. In these karst springs, partially captured for drinking water supply, the recurrent turbid groundwater episodes suppose an important limitation for groundwater exploitation during several days, but also a concerning human health risk. The results revealed the different flow and sediment dynamics and mixing processes which determine the impact of faecal contamination derived from human activities on the karst groundwater drained by each spring. The described processes control the variable influence of allogenic recharge, which provokes notable differences regarding response times and maximum values of turbidity and associated bacterial activity in the investigated outlets. The outcomes of this work highlight the usefulness of the applied methodological framework to set the bases for an efficient implementation of early-warning strategies to prevent public health issues worldwide.

* Corresponding author.
E-mail address: jaimeortega@uma.es (J. Fernández-Ortega).

https://doi.org/10.1016/j.scitotenv.2023.169539
Received 7 September 2023; Received in revised form 12 November 2023; Accepted 18 December 2023
Available online 22 December 2023

1. Introduction

Carbonate rocks cover about 12 % of the global land surface and a recent estimation revealed that approximately 678 million people (9.2 % of the total world population) are supplied by drinking water from aquifers developed in such type of karstifiable lithologies (Stevanović, 2019). In Europe, about 5.1 % of the territory consists of continuous carbonate rock exposures, in addition to 6.5 % comprising discontinuous karst (Chen et al., 2017). In some countries, such as Austria or Slovenia, approximately half of the drinking water supply comes from carbonate aquifers. The dependence on karst groundwater resources is predominant or total in large cities worldwide such as Montpellier (France), Rome (Italy), Vienna (Austria), San Antonio (USA), Damascus (Syria), Beirut (Lebanon) or Taiyuan (China) (Kresic and Stevanovic, 2010; Chen et al., 2017).

Due to inherent hydrogeological features of karst aquifers, which favour the quick arrival of a potential pollutant entering the system with little natural attenuation, the risk of suffering a contamination event at drinking water sources is enhanced, making these types of media highly vulnerable to contamination (White, 1988, Goldscheider, 2005). Faecal bacteria from domestic sewage leakages (USEPA, 1986; Buckerfield et al., 2020), individual septic tanks (Hagedorn, 1984), wastewater treatment plants (Reed et al., 1988) or associated to the application of manure and cattle pasturing (Drew and Hötzl, 1999; Boyer and Pasquarell, 1999) constitute most of the common threats to karst groundwater in urban and rural environments. Moreover, the transfer of faecal contamination through karst aquifers is usually enhanced by other factors (e.g. sediment transport, organic matter load). Mobilization of suspended particles (which is well known in karst aquifers and causes quick turbidity variations) may act as a vector for the transport of bacteria during episodes of intense rain (Mahler et al., 2000), so their presence in capture points intended for drinking water supply may have direct implications for health. Given that wells and springs constitute the main sources of drinking water in karst regions, contamination events commonly result in repeated interruption of groundwater exploitation for urban supply (Beaudeau et al., 2012).

Protection of groundwater and drinking water sources constitutes a major priority for drinking water companies and public administrations to avoid health risks (Foster et al., 2002). Due to their high vulnerability and heterogeneity, karst systems require specific investigation methods and management tools across all scales, which range from catchment to karst aquifer or springs and wells (Goldscheider and Drew, 2007). Such tools include vulnerability mapping, delimitation of protection areas or inventory of contaminant pressures (Goldscheider, 2005; Marín et al., 2021). The quick variations of chemical quality observed in karst springs demonstrate the need of developing real-time monitoring and predictive systems to minimize the risk of contamination of drinking water sources to protect human health.

Real-time monitoring of karst groundwater parameters coupled to an automatic data transmission and process analysis (the so-called Early Warning Systems -EWS-; Storey et al., 2011) have emerged as a powerful tool for water managers to rapidly detect contamination episodes in drinking water sources. In the last decades, continuous water parameters have been tested to correlate with pollutants (or associated transport vectors) with special focus on faecal contamination given the time-consuming analysis to determine their presence through classic laboratory methods. Some of those parameters or techniques are spring discharge (Auckenthaler et al., 2002), turbidity (Ryan and Meiman, 1996; Massei et al., 2003), organic carbon (Pronk et al., 2007; Frank et al., 2022) or fluorescence-based techniques (Sorensen et al., 2015), among many others. However, some of these studies focused on time series analysis, correlation between basic and key-specific parameters during a single flooding event and do not provide a robust conceptual model of the occurrence of contamination events. Thereby, long-term karst-specific hydrogeological researches are required to understand the complex interaction between karst aquifer, contaminant sources and factors that control their transport mechanisms and attenuation in groundwater. A comprehensive knowledge of these elements is essential to develop the optimal early-warning strategies for each karst system (Storey et al., 2011; Cuk Đurovic et al., 2022; Ravbar et al., 2023).

In this research, a set of karst spring floodings has been analysed at event scale, focusing on turbidity variations with associated inorganic and organic compounds as well as bacteriological contaminants. This work aims to advance in the development of early-warning strategies by testing the reliability of the proposed methodological approach for real-time detection of insufficient karst groundwater quality periods for human consumption through the construction of a robust conceptual model of contaminant transfer. Specifically, this research pursues (i) to increase risk awareness by identifying the main contaminant sources derived from human activities; (ii) to acquire a comprehensive insight about the physical processes responsible for the occurrence of turbidity episodes and its implications in the transport of pathogen organisms; and (iii) to provide new insights on the development of early-warning strategies in karst systems.

2. Test site description

2.1. Location and climate

Sierra de Ubrique aquifer (Fig. 1) constitutes a 26.06 km^2 mountainous area in the surroundings of Sierra de Grazalema Natural Park (Cádiz province, S Spain; Fig. 1A, B), located approximately 80 km NE from Cádiz city. The topography of this area presents a set of NE-SW mountainous reliefs with abrupt terrain elevations that range between 400 and 1395 m a.s.l. with steep slopes (Marín et al., 2021). The study area presents hot summer Mediterranean climate (Csa) (Geiger, 1954) and it's characterized by a marked seasonal pattern with a rainy period in winter and a long-lasting dry summer (null rainfall). The closeness of this area to the Atlantic Ocean (80 km, Fig. 1A) results in a mean annual precipitation and air temperature values of 1305 mm and 14.8 °C respectively (period 1984/85 to 2017/18, Martín-Rodríguez et al., 2023). The great pluviometry in this area is due to the position of Sierra de Grazalema in the NE part of Cádiz province (Fig. 1B) as it constitutes the first great orographic barrier against the humid Atlantic cloud fronts.

2.2. Geology and karst geomorphology

The study area belongs to the External Zone of the Betic alpine orogen and is mainly characterized by Upper Triassic (Keuper) clays with evaporites, Jurassic dolostones and limestones and −500 m thick-, and Cretaceous-Paleogene marls and marly-limestones (Martín-Algarra, 1987). The geological structure is defined by anticline folds (Sierra de Ubrique and Sierra del Caíllo; Fig. 1C), in which hinge Jurassic limestones and dolostones crop out, and synclines matching with land depressions hosted by Cretaceous marls and marly-limestones. Furthermore, Tertiary clay and sandstone formations (the so-called Flysch del Campo de Gibraltar) overthrust all the Mesozoic rock sequence. Recent strike-slip fault (NW-SE) and normal fracture (NNW-SSW and N-S) networks mainly comprises the tectonic setting of the area (Martín-Algarra, 1987).

The abundance of highly fractured Jurassic oolitic limestones, together with the bedding planes orientation (almost horizontal) and the current climate conditions, favour the development of karstification processes which gives rise to exokarst landforms (karrenfields, poljes, dolines, uvalas) over the bare carbonate outcrops (Martín-Rodríguez et al., 2023). Furthermore, the presence of low-permeability rocks (marls and clays) at the bottom of valleys leads to the development of endorreic areas (such as Albarrán stream catchment, Fig. 1C). These land depressions are in close connection to subsurface through swallow holes, shafts and other endokarst features like siphons and large conduits partially explored by speleologists (Mendoza, 1992).

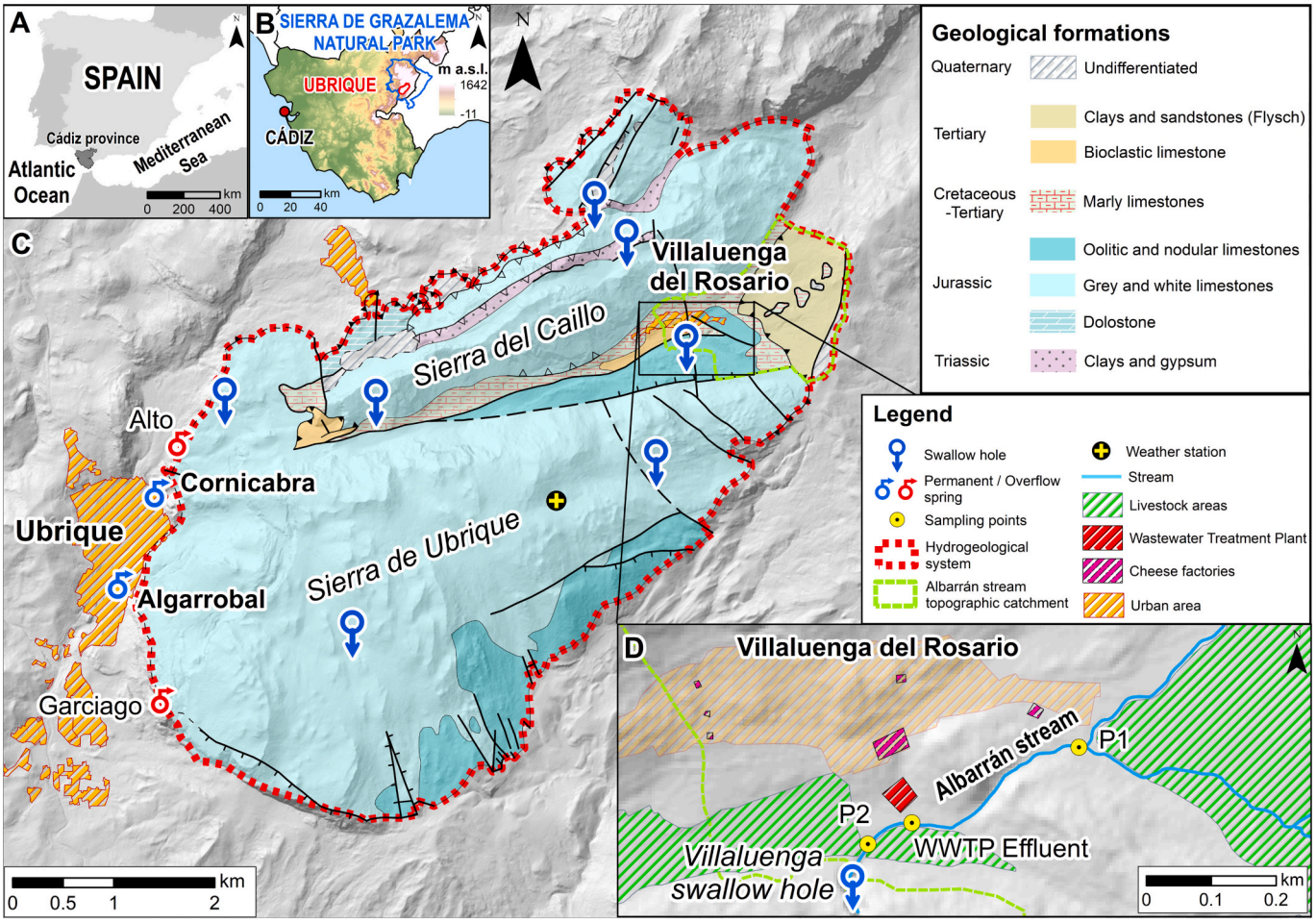

Fig. 1. A) Location of the study area, B) location of the study area within Cádiz province, C) hydrogeological setting of the study area, D) hydrogeological setting of the Villaluenga swallow hole environment.

2.3. Hydrogeology

Recharge in Sierra de Ubrique aquifer occurs twofold: (1) by diffuse infiltration from rainfall through carbonate outcrops (autogenic component) and (2) by concentrated flow mainly from a neighbour surface catchment (allogenic component) (Fig. 1D). Additionally, other small endorreic areas can be found in the syncline valley -between both sierras- as well as in the uplands of Sierra del Caillo and Sierra de Ubrique (Fig. 1C). The most important allogenic input comes from the Albarrán stream catchment, which sinks through the Villaluenga swallow hole (Fig. 1D). It has an effective surface of 2.03 km^2 and is composed by Cretaceous marly limestones and clays and sandstones from the Flysch formations (Martín-Rodríguez et al., 2023). The activation of this stream highly depends on the runoff generation, leading to intermittent surface water inflow through the swallow hole, which can rapidly rise from 0 to 4.000 L/s in a few minutes during an intense storm event.

Natural drainage of Sierra de Ubrique aquifer is produced through the permanent and temporal (overflow) springs located in its SW border (Fig. 1C), the most significant ones are the Cornicabra (349 m a.s.l.) and Algarrobal (317 m a.s.l.) perennial outlets (Martín-Rodríguez et al., 2023), which have discharge rates of 20–1604 L/s (average 270 L/s) and 20 to 828 L/s (average 372 L/s), respectively during the study period. Additionally, several overflow springs appear in the NW edge (towards the N of Cornicabra spring: Alto, 521 m a.s.l.) during flooding events (Sánchez et al., 2018); and to the S of Algarrobal, Garciago spring, (422 m a.s.l.) which ranges from 0 to 5042 L/s. Water quality issues dealing with high turbidity levels were observed in such springs (Martín-Rodríguez et al., 2023; Marín et al., 2021) but those investigations did not go further in the detailed description of the occurrence of contamination events.

The principal hydrogeological karst connections were proved by the performance of two tracer tests (Martín-Rodríguez et al., 2023) that allowed the identification of the main groundwater flow routes within the studied aquifer. Such field experiments also provided valuable information about response times (31 h in Cornicabra, 47 h in Algarrobal and 35 h in Garciago) and the estimation of the allogenic recharge contribution through Villaluenga swallow hole. Recovery rates of the tracer injected at that point resulted in 2 % in Cornicabra, 21.9 % in Algarrobal and 68.4 % in Garciago springs.

2.4. Anthropogenic pressures

Over the recharge area of the Sierra de Ubrique aquifer, different pressures to karst groundwater were identified related to rural activities developed in the small population of Villaluenga del Rosario (500 inhabitants) (Fig. 1D). Those are cow, goat and sheep livestock, several small cheese factories and a wastewater treatment plant (WWTP), which sewage is directly released into the Albarrán stream where liquid and solid wastes are accumulated along small ponds most of time. Despite that part of the milk whey volume produced at the cheese factories is taken to a specific treatment plant, along the study period, its spill into the catch basin of the sewage system was recurrent. Deficiencies in the water treatment have been reported in a recent report (Junta de

Andalucía, 2021) of the water agency. This publication indicates that the WWTP of Villaluenga del Rosario village receives whey from the processes related to the town's food industry and presents a poor treatment caused by a process design that does not fulfil the required quality characteristics of the effluent regarding Biochemical Oxygen Demand (BOD) and Total Nitrogen.

3. Material and methods

3.1. Monitoring strategy

The study period comprises two complete water years, from 01/10/2020 to 30/9/2022. The monitoring network includes different sampling points to control (i) the permanent discharge through karst springs captured for drinking purposes, (ii) the allogenic recharge contribution, and (iii) hydroclimatic control in Sierra de Ubrique (Fig. 1C, D).

Discrete groundwater sampling was done in the perennial outlets (Cornicabra and Algarrobal) on average, daily at event scale, although was intensified each 4 h, with the support of automatic samplers ISCO 3700 (Teledyne™ ISCO, Lincoln, USA).

The sampling points in the main allogenic recharge area consist on the WWTP effluent as well as P1 and P2 in Albarrán stream, located upstream and downstream the effluent pipe, respectively (Fig. 1D). Sampling procedure in P1 and P2 was variable from daily to hourly periodicity but limited to the activation periods after rain events. WWTP effluent samples were taken approximately once a month (as close as possible to the output pipe).

3.2. Physico-chemical parameters and continuous records

Physico-chemical parameters (electrical conductivity -EC-, water temperature, pH, oxidation reduction potential -ORP- and turbidity) were measured in situ in the WWTP effluent, surface water and groundwater. Electrical conductivity and water temperature were measured using hand-held meter WTW™ Cond 3110 (Xylem Analytics Germany Sales GmbH & Co, Mainz, Germany) which presents a precision of ±0.5 % and ± 0.1 °C, respectively. The (HACH™, Loveland, USA) multiprobe HQ40D was used to obtain pH and ORP data with a precision of ±0.002 pH and ± 0.1 mv. Finally, the turbidity was determined through the use of a 2100Qis (HACH™, Loveland, USA) portable turbidimeter which presents a precision of ±2 % and a detection limit of 0.02 nephelometric turbidity units (NTU).

EC, water temperature, Tryptophan-Like-Fluorescence (TLF) and turbidity were continuously measured at 15 min intervals using a GGUN FL30® field fluorometer (Albillia Sàrl., Neuchâtel, Switzerland). The obtained records of EC, water temperature and turbidity were corrected using the data obtained from in-situ measurements. Likewise, the TLF record was calibrated with a L-tryptophan laboratory standard of analytical grade (CAS: 73–22-3; Sigma-Aldrich, Merck KGaA, Darmstadt, Germany).

Water level was as well measured at 15 min interval with an Odyssey® capacitance data loggers (Dataflow Systems Limited, Christchurch, New Zealand) and converted into spring discharge data through a rating curve developed in previous investigations (Martín-Rodríguez et al., 2023). Although meteorological stations of the Spanish Meteorology Agency (AEMET) were available in the surroundings of the study area, a weather station Davis Vantage Pro™ for hourly measurement of rainfall was installed at Sierra de Ubrique (Fig. 1C), at an altitude of 1029 m a.s.l.

3.3. Total organic carbon and N-compounds

Water and WWTP effluent samples were taken directly at the Albarrán stream, output pipe and springs and then immediately stored in 125 mL dark glass vials and refrigerated in the dark after their collection. Groundwater samples taken with autosampler were collected no later than 12 h after taking the sample to avoid an excessive modification of their chemical properties. Hand-taken and water samples from automatic sampler were taken to the CEHIUMA laboratory within 48 h after sampling for the analytical determinations.

N-compounds (NO_3^- and NO_2^- and NH_4^+) were determined through ion chromatography using models 881 Compact IC pro and 792 Basic IC (Metrohm®, Herisau, Switzerland) with 2 % resolution. The quality of major ions data was assessed using the Charge Balance Error (CBE). The mean CBE value for the whole sample set was 0.5 % and groundwater samples with CBE higher than ±5 % were not considered. The determination of Total Organic Carbon -TOC- was carried out with a TOC-V_{CSN} analyser (Shimadzu®, Kyoto, Japan). The analytic method of this equipment is based in oxidation by catalytic combustion of organic matter at 680 °C.

3.4. Bacterial activity

Duplicate samples were used to determine bacterial activity within 12 h after sampling. Microbiological determination was only done in hand-taken samples since the cross-contamination of the samples is highly probable in automatic samplers. Total Coliforms (TC) and *Escherichia coli* (*E. coli*, which is widely accepted as faecal indicator) were analysed as the Most Probable Number (MPN) per 100 mL following the Colisure-Quanty-Tray/2000 method (IDEXX™ Laboratories Inc., Westbrook, USA). The microbial quantification range of this testing technique is from 1 to 2419 MPN/100 mL and method failure rate was determined to 20 % by Olstadt et al. (2007). Where an exceedance of this value was expected, the samples were diluted with ultrapure water.

3.5. Statistical analysis

The correlation analysis applied in this research includes the determination of cross-correlation functions (CCF) in the time domain, which has been widely used in karst hydrogeology (e.g., Padilla and Pulido-Bosch, 1995; among many others). This bivariate analysis was used to determine the relationship between two discretized series: input series (precipitation) and the output series (spring discharge, turbidity and TLF). To identify the most relevant proxy parameters, linear regression analysis has been performed and Spearman correlation coefficients (*p;* Zar, 2008) were obtained considering physico-chemical continuous parameters (EC, water temperature, turbidity, TLF) and contamination related parameters (TC, *E. coli*, TOC, NO_3^- and NO_2^-) obtained from the laboratory determinations. RStudio (R Core Team, 2021) was used for Cross-correlated functions (CCF) and Spearman's correlation coefficients (*p*) statistical analysis.

4. Results

4.1. Characteristics of flooding events

Accumulated rainfall and hydrodynamic variations recorded at the main permanent outlets (Cornicabra and Algarrobal) are represented in Fig. 2. Although numerous precipitation episodes occurred during the study period, only a few were of enough magnitude and intensity to produce significant hydrodynamic responses at the springs. As an example, previous precipitation episodes to Event 1 (E1, in Fig. 2) didn't produce any change in spring discharge (except for the minor spring discharge increase in Cornicabra) despite that the maximum intensity was up to 16 mm/h. A similar situation was observed after E5, at the end of the dry season (low flow conditions), with a maximum rain intensity of 17.1 mm/h that only produced a significant hydrodynamic variation in Cornicabra spring.

The main hydroclimatic parameters together with hydrodynamic variables used to describe selected flooding events in Cornicabra and Algarrobal springs are summarized in Table 1. Two flooding events (E1

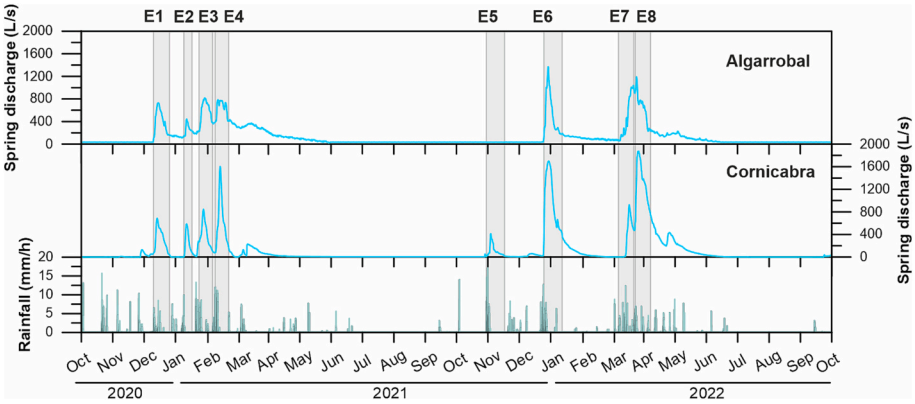

Fig. 2. Time series of rainfall and spring discharge at Cornicabra and Algarrobal from October 2020 to October 2022.

Table 1
Summary of the main climatic and hydrogeological characteristics (total rainfall, event duration, maximum rain intensity, days since the last event, initial discharge, maximum discharge and maximum turbidity) of selected flooding events at the studied permanent springs.

Event	Total rainfall (mm)	Event duration (hour)	Maximum intensity (mm/h)	Days since the last event >70 mm	Pre-event discharge (L/s)		Maximum discharge (L/s)	
					Cornicabra	Algarrobal	Cornicabra	Algarrobal
E1	154	114	8.5	320	15	32	645	739
E2	72	75	9.9	23	21	106	661	468
E3	256	143	13.3	11	24	169	1454	828
E4	288	132	12	10	79	404	1770	792
E5	357	91	17.1	260	11	33	410	35
E6	286	147	12.7	49	21	49	1699	1513
E7	188	85	12.4	75	13	238	924	1167
E8	173	71	7	6	471	945	1874	1363

and E5) highlight after the longest time elapsed since the last precipitation event with an accumulation >70 mm. This value matches the minimum accumulated rainfall that produced a hydrodynamic response in this research (e.g. E2, in Table 1). Pre-event hydrodynamic conditions (Table 1 and Fig. 2) were quite variable according to the elapsed time since the last effective recharge event. Hence, the first flooding event of the hydrological year (E1 and E5) presented the lowest pre-event discharge values in both Cornicabra (11–15 L/s, Table 1) and Algarrobal springs (32–33 L/s).

The flooding events produced at the studied springs after stormy rains (Table 1) result in the drainage of turbid groundwater (>4 NTU, the maximum threshold in the Spanish law (RD 3/2023, 2023); Figs. 3 and 4), which frequently force the interruption of the water capture system for urban supply at Ubrique town during several days.

4.2. Physico-chemical database at selected sampling points

The main statistics of hydrodynamic and physico-chemical parameters measured in the field as well as of the chemical and microbiological analyses from laboratory determinations are summarized in Table 2. The number of runoff flow measurements is limited and only representative of the Albarrán stream activation periods during precipitation episodes. Thus, mean surface flow values obtained at the two reference points (P1 and P2; see point location in Fig. 1D) are quite similar. The contribution of the WWTP effluent is negligible in terms of discharge (~0.2 L/s was estimated in the field) during rain events, but it represents the only water input to Albarrán stream during low flow periods. Mean discharge and variability in Ubrique springs show a similar magnitude during the study period, although it is roughly greater in Algarrobal compared to Cornicabra (Table 2). Regarding peak discharge, maximum value recorded was slightly higher in Cornicabra spring.

The WWTP effluent samples have relatively high mineralization (Table 2) but also a high variability in the chemical composition. Surface water samples at P1 and P2 display EC variations within a similar range to those found at Cornicabra (267 μS/cm) and Algarrobal springs (324 μS/cm). Maximum turbidity values registered at runoff waters are comparable to those measured in Algarrobal spring (334 NTU), which is one order of magnitude higher than Cornicabra spring.

Multiple dilutions (ten to hundred times) were required for the chemical analysis of WWTP effluent samples, which show the highest mean and maximum TOC concentration (Table 2) among all sampling points. Although mean TOC content in Albarrán stream is slightly higher in P2 than in P1, the maximum value measured in P2 (26.9 mg/L) is considerably higher than that measured in P1 (9.2 mg/L). Both samples that account for the maximum TOC values in runoff were taken on November 5, 2020 during one of the first rain events of the hydrological year. In both karst springs, a mean TOC concentration below 1 mg/L was measured while maximum value in Algarrobal spring was found to be twice the highest value of Cornicabra (Table 2).

As shown in Table 2, the semiquantitative estimation of bacterial load in WWTP effluent and runoff samples reached the upper limit of method quantification (>2419 MPN), even after water sample dilution by 10^6 times. Bacterial activity measurements at Cornicabra spring show a Total Coliforms maximum of 1553 MPN/100 mL and 2978 MPN/100 mL at Algarrobal (obtained from 1:2 and 1:10 dilutions), while *E. coli* counting reached a maximum of 920 MPN/100 mL and 1732 MPN/100 mL, respectively.

The concentration of N-compounds shows remarkable differences among sampling points (Table 2). Measurements of WWTP effluent samples especially highlight due to the major presence of reduced species such as NH_4^+ and NO_2^-. In contrast, a higher concentration of N-oxidized species is predominantly found in runoff samples, with higher mean concentration of NO_3^- in P1 compared to P2, although the maximum values were found in the downstream point. At the karst springs, mean NO_3^- contents don't exceed 4 mg/L (Table 2), but maximum values are up to 7.9 mg/L in Cornicabra and 12.2 mg/L in Algarrobal. NO_2^- was only detected in 24 % of the taken samples in Cornicabra and 30 % in Algarrobal spring.

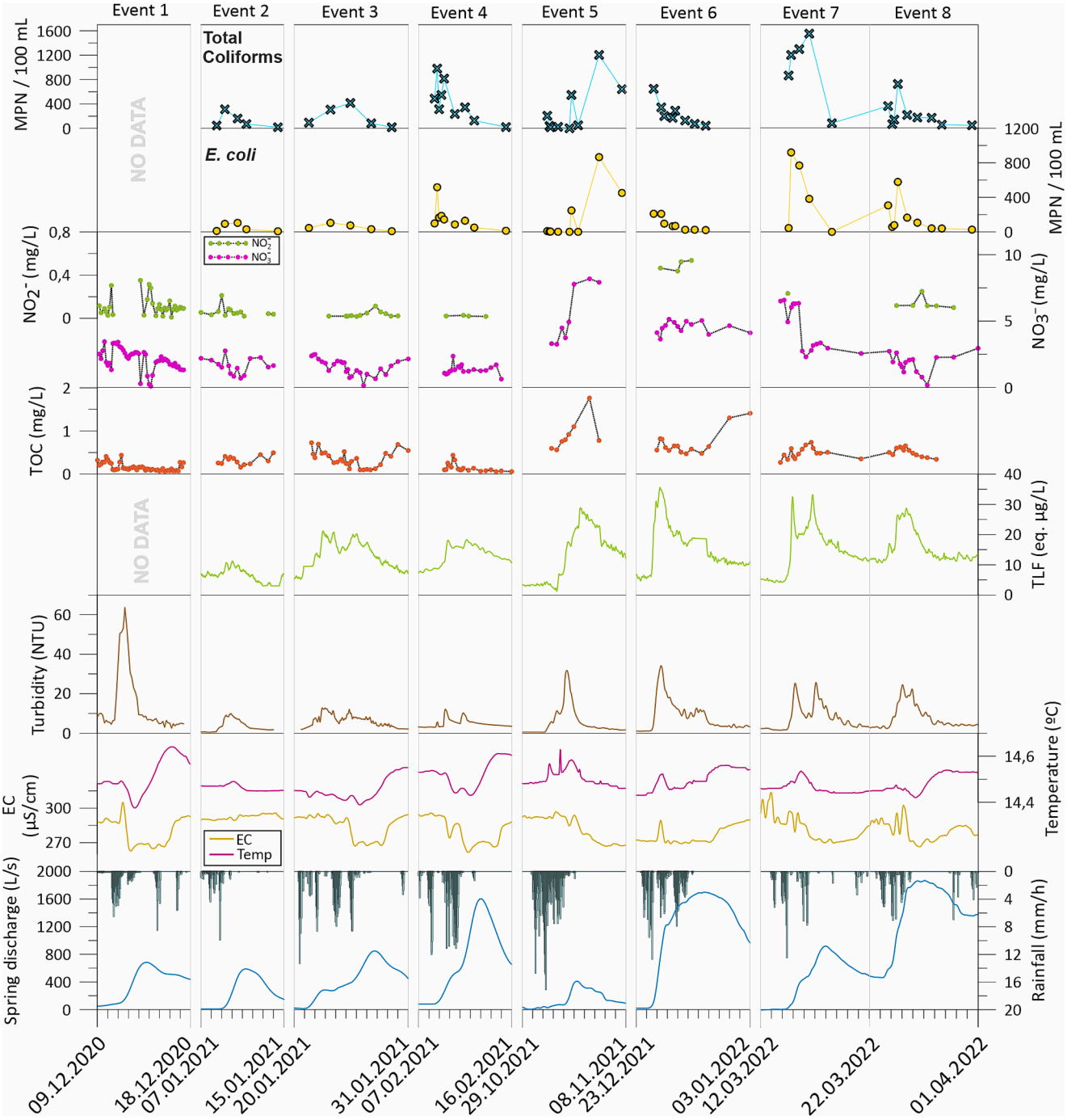

Fig. 3. Time series (event scale) of rainfall, spring discharge, physico-chemical parameters, and bacterial activity indicators in Cornicabra spring water.

4.3. Spring responses to individual rain events

4.3.1. Cornicabra spring

The individual flooding events (Fig. 3) show maximum discharge in the range 800–1800 L/s and fast hydrodynamic responses to precipitation events. In general, the flooding period lasts approximately 7–14 days, after which spring discharge returns to pre-event values. The EC record in Cornicabra spring depicts peaks (>300 µS/cm) at the beginning of the flooding event followed by a dilution interval (except in E2). Spring water dilutions show EC values <270 µS/cm and normally coincide with discharge rates >400 L/s (Fig. 3).

Turbidity and TLF records display quick and proportional increases with spring discharge at the beginning of the flooding event. In flow conditions between 100 and 1000 L/s; (Events 2 to 8, Fig. 3), groundwater drained by Cornicabra spring normally shows the highest turbidity and TLF values (>20 NTU and > 20 eq. µg/L), coinciding with the rising limb of the spring hydrograph. TLF reaches maximum values between 20 and 35 eq. µg/L usually concomitant to turbidity peaks (Fig. 3). Once the maximum spring discharge has been reached, relative maximums of turbidity (~ 6–10 NTU) are registered. This parameter showed the maximum value (64 NTU) at the beginning the first flooding event in 2020 (Event 1, Fig. 3) and this value was not registered later independently from the magnitude of the rain episodes (e.g., Event 2 to 5, Table 1). During the next two hydrological years, the successive flooding events showed multiple turbidity peaks and relative maximums that do not exceed 13 NTU (2020/21) and 34 NTU (2021/22).

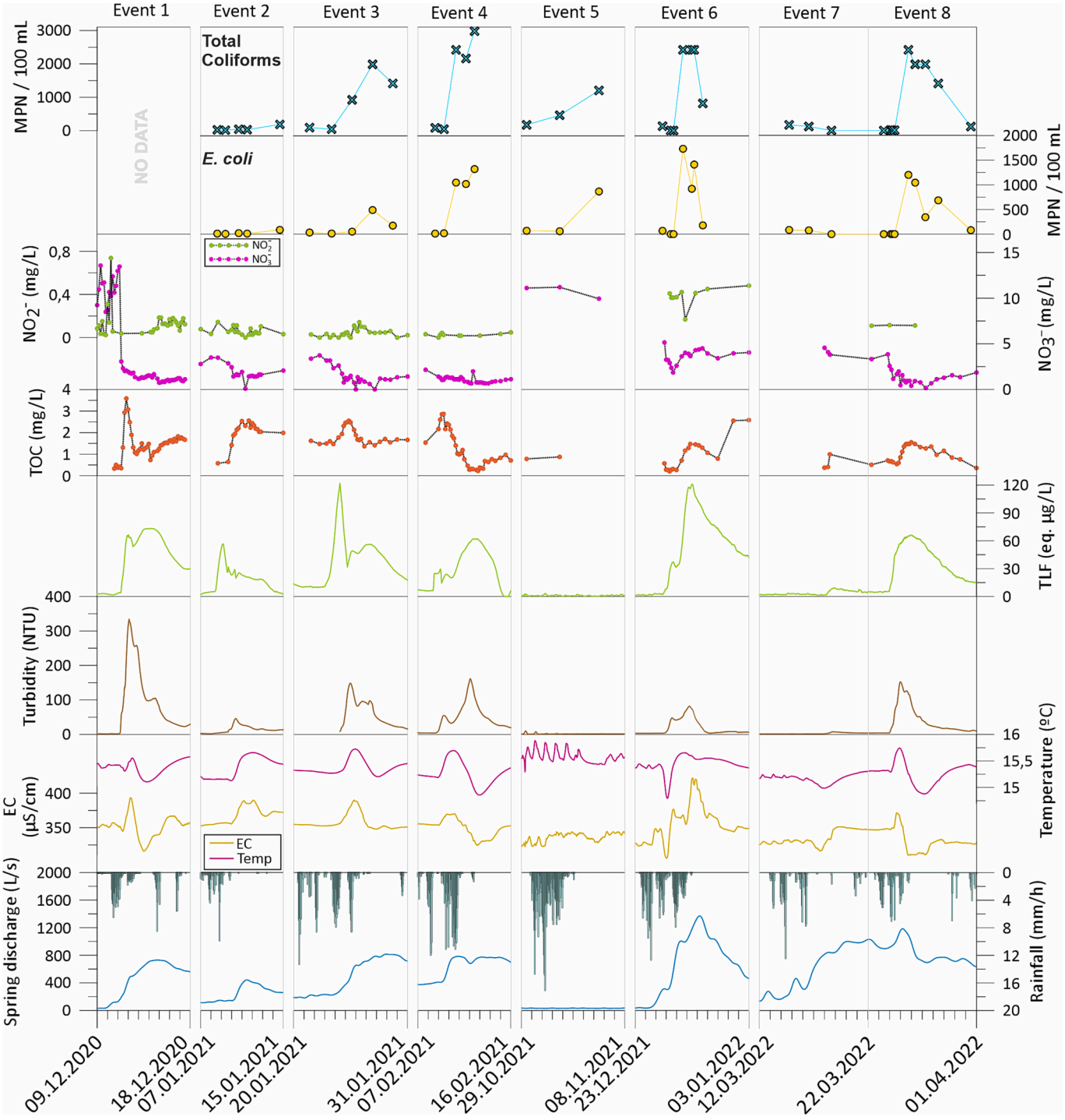

Fig. 4. Time series (event scale) of rainfall, spring discharge, physico-chemical parameters, and bacterial activity indicators in Algarrobal spring water.

TOC measurements depict variations between 0.3 and 1 mg/L, except for Event 5, which shows the maximum value. TOC record sometimes presents successive relative maximums that apparently do not correlate with turbidity and TLF or evidence an enrichment at the end of the flooding event (Events 3, 5 and 6; Fig. 3).

The variations of N-compounds are normally marked by (1) a decrease of NO_3^- that in some cases (Events 3 and 8) reaches 0.4 mg/L and (2) a rising in NO_2^- concentration (up to approximately 0.2–0.3 mg/L), directly related to variations of spring discharge (e.g., Events 1 and 7; Fig. 3). In the case of Event 5, the exceptional increase of NO_3^- content is on the order of 20 times while NO_2^- was not detected. NH_4^+ was not detected in Cornicabra spring.

Bacterial indicators display different changes depending on the flooding event: Events 2, 4, 6, 7 and 8 show maximum bacterial activity at the beginning of the flood and then they decrease. On the contrary, flooding Events 3 and 5 depict an increasing bacterial activity towards the end of the event. Thus, the maximum number of TC and *E. coli* is found during intermediate flow conditions and it decreases with higher spring discharge rates.

4.3.2. *Algarrobal spring*

The analysis of the same flooding events in Algarrobal spring (Fig. 4)

Table 2
Statistics for electrical conductivity, water temperature, turbidity, pH and ORP data in WWTP effluent, runoff from Albarrán stream (both monitoring sites) and permanent karst springs waters. Acronyms: number of measurements (n), maximum (max), minimum (min), mean and standard deviation (SD). Marks: *Estimated from field observations; **Data from continuous record of field devices; ***Upper quantification limit of the MPN method for *E. coli* determination.

		WWTP effluent	Albarran stream (P1)	Albarran stream (P2)	Cornicabra spring		Algarrobal spring	
	Altitude (m a.s.l.)	826	848	819	349		317	
Flow/spring discharge (L/s)	n	0	5	7	16195**		16212**	
	Max	0.2*	2450	2770	1874		1513	
	Min		118	220	5		27	
	Mean		1033	929	228		280	
	SD		1049	949	365		243	
Electrical Conductivity (µS/cm)	n	16	8	30	15563**	62	15642**	54
	Max	5350	353	418	305	295	424	408
	Min	410	156	126	261	227	242	256
	Mean	1293	232	237	287	267	317	325
	SD	1272	65	64	9	13	22	34
Temperature (°C)	Max	20.3	12.5	17.2	14.6	14.6	15.8	15.4
	Min	9.8	9	7.2	14.4	14.1	14.8	14.3
	Mean	14.1	11.1	11.3	14.5	14.4	15.3	14.8
	SD	3.1	1.3	2.1	0.1	0.1	0.2	0.3
Turbidity (NTU)	Max	487	259	334.3	63.7	30.7	334.2	144
	Min	15.1	2.21	6.1	0.4	0.42	0.7	0.2
	Mean	139.0	24.1	78.9	3.4	6.8	14.7	25.6
	SD	124.9	92.5	87.3	2.8	7.0	26.5	34.3
TLF (eq. µg·L^{-1})	Max	No data				34.8		119.7
	Min					3.38		1.1
	Mean					15.6		26.1
	SD					7.9		29.1
pH	Max	9.0	8.6	8.8		8.1		8.3
	Min	7.1	7.3	7.4		6.7		6.6
	Mean	7.8	8.1	8.3		7.5		7.5
	SD	0.5	0.4	0.3		0.3		0.4
ORP (mv)	Max	242	247	472		298		338
	Min	−298	15	39		−22		−7
	Mean	−47	31	146		103		117
	SD	202	93	101		83		97
TOC (mg/L)	n	16	8	30		62		54
	Max	3671	9.2	26.9		1.4		2.9
	Min	15.2	2.7	2.6		0.1		0.1
	Mean	759.4	5.6	6.5		0.4		0.8
	SD	1217.7	2.2	4.9		0.3		0.7
Total Coliforms (MPN/100 mL)	Max	>2419***	>2419***	>2419***		1553		2978
	Min	Over method upper detection limit				1		1
	Mean					284		629
	SD					440		931
E. coli (MPN/100 mL)	Max	>2419***	>2419***	>2419***		920		1732
	Min	Over method upper detection limit				1		1
	Mean					105.0		269.3
	SD					212.4		460.1
NO_3^- (mg/L)	Max	2.1	8.2	14.6		7.9		12.2
	Min	0.1	1.5	0.1		0.4		0.4
	Mean	0.7	3.5	1.9		3.3		3.9
	SD	0.7	2.2	3		1.8		3.3
NO_2^- (mg/L)	Max	6.6	0.6	1.3		0.3		0.8
	Min	0.1	0.1	0.1		0.1		0.1
	Mean	1.5	0.2	0.3		0.2		0.2
	SD	2.3	0.2	0.3		0.1		0.2
NH_4^+ (mg/L)	Max	23.9	Below method detection limit					
	Min	0.1						
	Mean	11.2						
	SD	11.1						

displays quick discharge variations from 100 to 800 L/s during hydrological year 2020/21 (Events 1 to 4), reaching higher flow rates of 1600 L/s in the water year 2021/2022 (Events 6 and 7). EC time series values evolve, to a greater extent, twofold (Fig. 4): i) an increase in groundwater mineralization (of up to 400 µS/cm) is registered that thereafter returns to the pre-event values (≈350 µS/cm; Events 2 and 3); otherwise, ii) a similar increase of EC is followed by a water dilution (down to 300 µS/cm; Events 1 and 4).

Groundwater drained by Algarrobal spring generally shows turbidity rising simultaneous to discharge (Fig. 4), specially over 400 L/s, and displays maximum turbidity (334 NTU) during the first flooding event of 2020/21 water year (e.g. Event 1). In the following flooding events, turbidity peaks normally vary between 100 and 150 NTU, with relative maximums of lower magnitude (e.g., Events 3, 4 and 6; Fig. 4). The increases observed in TLF signal are roughly proportional to that of spring discharge at the beginning of the flooding event, as it can be seen in Events 1, 3, 6 and 7 (Fig. 4). However, anticipated increases of TLF respect to spring discharge were recorded in flooding Events 2 and 3, with an approximate time lag of 29 and 9 h. TOC contents usually reach maximum values in the first 48 h after spring discharge peak.

N-compounds follow the same pattern previously described in Cornicabra spring, although with a more pronounced variation in NO_3^-

concentrations (Fig. 4). As an example, in Event 1 NO_3^- content changes from 12 mg/L down to 2 mg/L. NO_2^- depicts narrower variations, from 0.02 to 0.2 mg/L (Events 2 and 3), linked to discharge variations. Furthermore, maximum NO_2^- concentration of 0.8 and 0.5 mg/L were found in events 1 and 6 respectively (Fig. 4). It specially highlights that, in Events 5 and 7, NO_2^- was not detected.

As a general observation (e.g. events 2, 4, 6 and 8; in Fig. 4), samples taken during the first moments of increasing turbidity have low TC and *E. coli* values (<10 MPN/100 mL) and a raising activity as the flooding event evolves (between 500 and 1000 MPN/100 mL of *E. coli* and 2500–3000 MPN/100 mL of TC). The maximum concentrations of TC and *E. coli* are found when spring discharge exceeds the discharge threshold of ca. 400 L/s.

4.4. Statistical analyses

4.4.1. Cross-correlation function (CCF)

The computed CCF between precipitation (P) and groundwater parameters (Q, Turb and TLF) for the two investigated karst springs and water years are represented in Fig. 5. All CCF (P vs Q-Turb-TLF) show a positive correlation (0.23–0.51, Table 3) with precipitation at both springs.

Cornicabra spring presents average response times for all the analysed parameters ranging from 19 to 92 h. The CCFs of P-Q display a certain similarity regarding the rounded and wide shape of the peaks and the greatest mean response times (Table 3) were found. In the water year 2020/21, the turbidity response precedes to that of the TLF by approximately 23 h, while in the following hydrological year the difference in response times between them occurs practically in a simultaneous way (Fig. 5). The P-TLF CCF have a wide shape with multiple relative maximum and mean response times between 32 and 42 h. The sharpest and narrowest peaks as well as the lowest mean response times (Table 3) are depicted by the P-Turb function. A time difference not higher than 24 h was found between P-Tub and P-TLF curves, which is substantially lower than time-lag estimated between spring discharge and turbidity (30h) and TLF (60 h) responses.

The individual CCFs obtained from Algarrobal spring display a similar shape to those obtained in Cornicabra spring for each parameter (Fig. 5), although they show slightly higher mean response times. Time gaps among curve peaks remain constant in both water years (Fig. 5).

Table 3
Summary of the results (cross correlation coefficient, R, and time lag) derived from the correlation analysis at Cornicabra and Algarrobal springs in both 2020/2021 and 2021/2022 water years.

		Cornicabra		Algarrobal	
	Correlation	R	Time lag (hour)	R	Time lag (hour)
20/21	P-Q	0.35	77	0.25	110
	P-Turb	0.27	19	0.36	35
	P-TLF	0.32	42	0.31	87
21/22	P-Q	0.27	92	0.24	120
	P-Turb	0.51	30	0.24	42
	P-TLF	0.23	32	0.25	98

4.4.2. Spearman correlation coefficients among parameters

Linear regression and correlation analysis between selected continuous parameters and laboratory analysis (Fig. 6) in groundwater samples from both permanent karst springs. Although data dispersion is also appreciated between the pairs of parameters, the statistical relationships are significantly stronger in Algarrobal spring. In Cornicabra spring, a reverse statistical correlation between EC and TLF is observed, as well as a positive relationship of turbidity with TLF, TC and *E. coli* (0.6). NO_3^- is the only compound that shows a negative correlation with the rest of the parameters in Algarrobal spring (Fig. 6), especially with turbidity, TLF and TOC. In that outlet, turbidity is significantly correlated with indicators of bacterial activity (0.6 for TC and 0.5 for *E. coli*). Furthermore, TLF shows better correlation with TC and *E. coli* and an apparent relationship with EC in Algarrobal spring waters.

5. Discussion

5.1. Human contamination sources

Due to its favourable conditions (pasture areas and accessibility with machinery), uplands of Albarrán stream catchment are normally used for extensive cattle activities, and thus, faecal remains are accumulated over the surface (Fig. 1D). Additionally, waste waters from the WWTP are constantly released into the Albarrán stream, although during dry periods the solid phase gets accumulated in the riverbed favoured by the strong evaporation in the environment. The organic matter input derived from human activities in the recharge area is mainly manifested

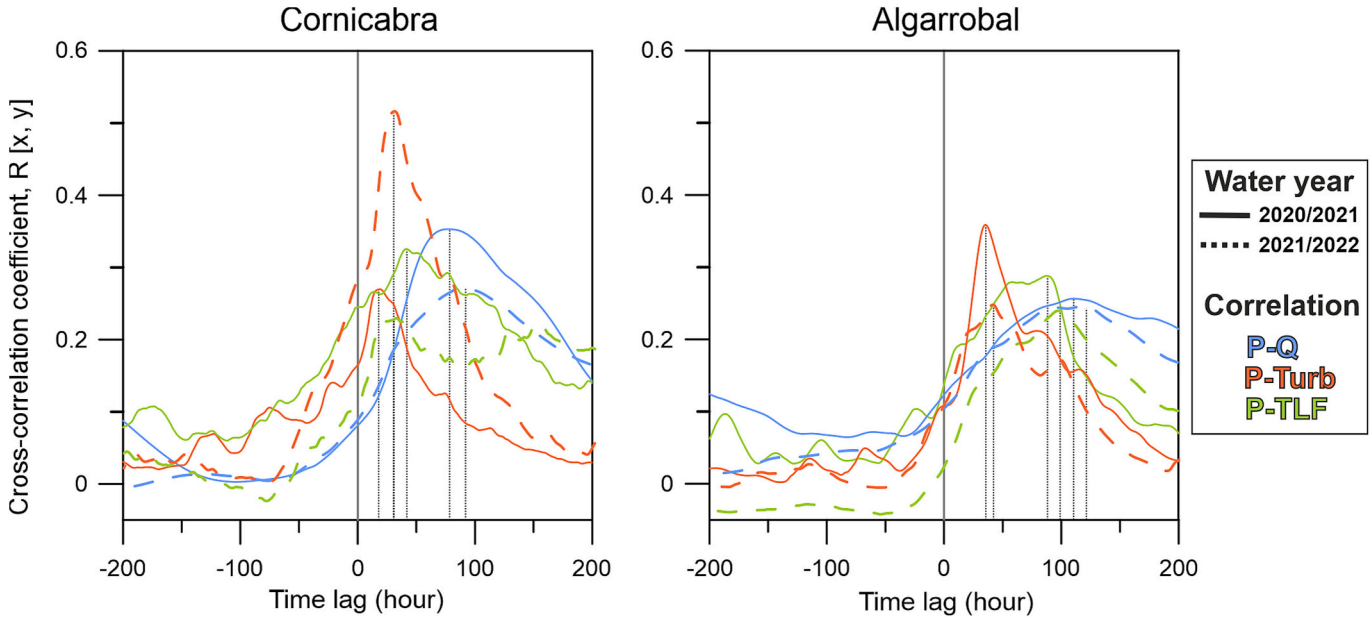

Fig. 5. Precipitation vs discharge, turbidity and TLF cross-correlation functions at both studied permanent karst springs and hydrological years.

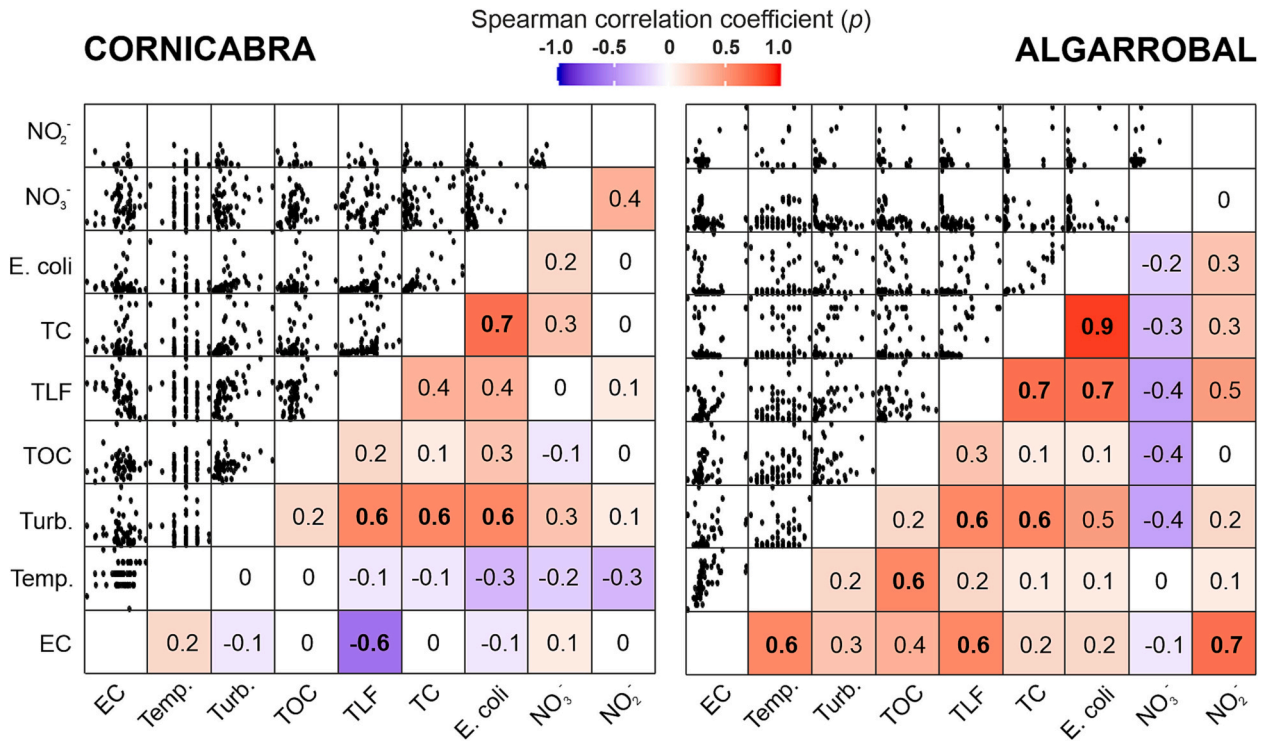

Fig. 6. Linear regression and Spearman correlation coefficients (Spearman's ρ) among continuous parameters (EC, temperature, turbidity, and TLF) and specific contaminant indicators (total coliforms -TC-, *E. coli*, TOC, NO_3^-, NO_2^-). Bold numbers indicate significant statistical correlations with $\rho > 0.6$ *or* $\rho < -0.6$.

in the significant increasing of TOC concentration from P1 to P2 surface water sampling points (Table 2).

Previous researches that applied analogous methodologies in karst springs with turbid groundwater affected by WWTP effluent inputs from rural populations (Heinz et al., 2009; Bicalho et al., 2012; Buckerfield et al., 2020) found comparable -although slightly higher- maximum activity of faecal bacteria (10^2–10^4 MPN/100 mL) and TOC concentrations (3–9 mg/L). A quantitative difference in terms of bacterial load is found in karst springs mainly affected by agricultural or livestock activities (Allocca et al., 2008; Epting et al., 2018; Buckerfield et al., 2020), which show maximum values of faecal bacteria of one order less of magnitude (300–900 MPN/100 mL).

ORP values measured in WWTP effluent samples suggest sufficiently anoxic conditions to reduce N-compounds through chemical processes induced by oxidation of organic matter. Li et al. (2010) found higher NH_4^+ and NO_2^- concentrations in sewage effluent and surface water than in groundwater affected by point pollution sources. Typically, dominant N species in karst groundwater is NO_3^- given its chemical stability (regarding oxidation/reduction processes) in highly oxygenated-turbulent flows and it is associated with a natural origin or comes from organic fertilizers (manure) used in agriculture or released in urban sewage (Musgrove et al., 2016; Nilsson and Widerlund, 2017; Yang et al., 2019). Turbulent flow through karst conduits provoke an increase of dissolved oxygen that might favour nitrification processes (Einsiedl and Mayer, 2006; Yang et al., 2020) and hence explains the low concentration of reduced N-species at the springs of Sierra de Ubrique aquifer.

Consequently, the WWTP constitutes the greatest impact to groundwater quality due to (1) the extremely high bacterial load of the effluent, (2) the low natural attenuation of the constant spill and (3) its location only 150 m far from the Villaluenga swallow hole. The research developed by Marín et al., 2021 stated the high vulnerability of the Sierra de Ubrique aquifer, but especially in the surrounding areas of the Albarrán stream endorheic catchment. Hydrogeological connections from Villaluenga swallow hole to both springs were already proved by qualitative dye tracing techniques (IGME, 1984); however, a major contribution of allogenic recharge to Algarrobal spring was demonstrated during intermediate-high flow conditions in a well monitored quantitative experiment (Martín-Rodríguez et al., 2023). All these previous results, put in evidence the need to implement protection strategies in Ubrique karst aquifer due to its exploitation for drinking water supply.

5.2. Contaminant transference in the binary karst system

5.2.1. Implications of sediment mobilization in faecal contamination

Turbidity is a physical property of water and cannot be considered as a contaminant. However, suspended sediments may act as a transport vector for bacteria (Mahler et al., 2000). Previous researches have demonstrated the survival potential of microorganisms when they are associated to particles because of the ability of bacteria to sorb onto them (Zobell, 1943; Palmateer et al., 1993; Pommepuy et al., 1992; Mahler and Lynch, 1999). In contrast, Sorensen et al. (2015) found a weak correlation ($p = 0.48$) between turbidity and *E. coli* and suggested that turbidity might be mainly generated by large particles while bacteria is transported when associated to smaller particles, such as DOM. The correlation obtained in this study between microbiological parameters and turbidity (0.6; in Fig. 6) suggests that suspended matter (such as particles) work as the main bacteria carrier in the aquifer. However, in the Algarrobal spring a good correlation was also obtained between TC and *E. coli* with TOC (0.6, in Fig. 6), which might suggest an enhanced role of organic substances in the transport of bacteria in karst systems with a high organic load. Therefore, an assessment of the sediment origin and subsurface transport modalities is crucial to determine its potential implications in contaminant arrival to the captured groundwater sources.

5.2.2. Relative contribution from allogenic recharge

Albarrán stream catchment and other small endorheic areas (Fig. 1C), where allogenic or concentrated recharge might occur during

a precipitation event, are primarily covered by highly weatherable *terra-rossa* and clayey materials (such as Flysch formations). The mobilization of sediments from these upland catchment locations is commonly promoted by heavy runoff eroding the soil horizon (Herman et al., 2012). Field observations in Albarrán stream catchment revealed that runoff is usually produced during >5 mm/h rain events. Surface flow activation provokes the releasing of a high amount of particulate materials to Albarrán stream (but also in many other ephemeral streams that drain smaller - <0.2 km^2 - endorheic catchments; Fig. 7B) resulting in quite high turbidity in runoff waters (Table 2). The upland catchments where these sinking rivers exist, flow rates of 10–100 L/s and turbidity values between 20 and 50 NTU were in-situ measured.

Several authors (Mahler et al., 1998; Massei et al., 2003; Pronk et al., 2007; Herman et al., 2008; Goldscheider et al., 2010; Jukić and Denić-Jukić, 2023) have described the predominant allochthonous (exokarstic) origin of suspended sediments in binary or fluviokarstic systems worldwide. In this way, the greatest contribution of suspended sediments to the Sierra de Ubrique carbonate karst aquifer occurs through the Villaluenga swallow hole due to the surface of the Albarrán stream catchment (relatively large compared to other endorheic areas) and, consequently, high runoff flow rates and sediment availability. In addition, its location in one of the highest (826 m a.s.l.) parts of the valley between the two carbonate massifs (Sierra del Caíllo and Sierra de Ubrique; Fig. 1C, D); and the intense rainfall episodes over a relatively steep slope in Albarrán stream catchment (13 % of mean slope) -able to generate maximum flow rates of up to 2770 L/s (Table 2)-, constitute determining factors in the sediment contribution to the system. Besides, the concentrated recharge via small swallow holes in the upper parts of the recharge area, which hydrogeological connection was previously proved (Martín-Rodríguez et al., 2023), must be also significant given its spatial distribution over the carbonate bare rocks (Fig. 1C).

5.2.3. *Sediment storage and mixing processes*

In Sierra de Ubrique karst system, the lack of proportionality observed between the total accumulation and/or maximum intensity of rainfall with spring discharge (at both permanent outlets) and turbidity (e.g. Event 1 compared to Event 5) suggests that mobilized sediments are washed into the conduit network and a fraction of those might be stored within the karst system. This non-linear pattern implies that, in addition to the sediment input from allogenic recharge and increases/decreases of the hydraulic head (Martín-Rodriguez et al., 2019), turbidity variations registered at the water sources also depend on the sediment availability within the karst conduits and mixing processes with diffuse recharge. To better illustrate the mixing processes which define each spring response, a conceptual model synthesizing key results is presented (Fig. 7A, B), with especial focus on contaminant transport in selected karst connections.

The cross-correlation analysis of the continuous records in Algarrobal spring displays a notable time-lag in P-TLF and P-Q functions compared to P-Turb (Fig. 5). Considering that the main source of organic compounds in karst groundwater comes from the concentrated recharge (Albarrán sinking stream and WWTP effluent), the significantly late

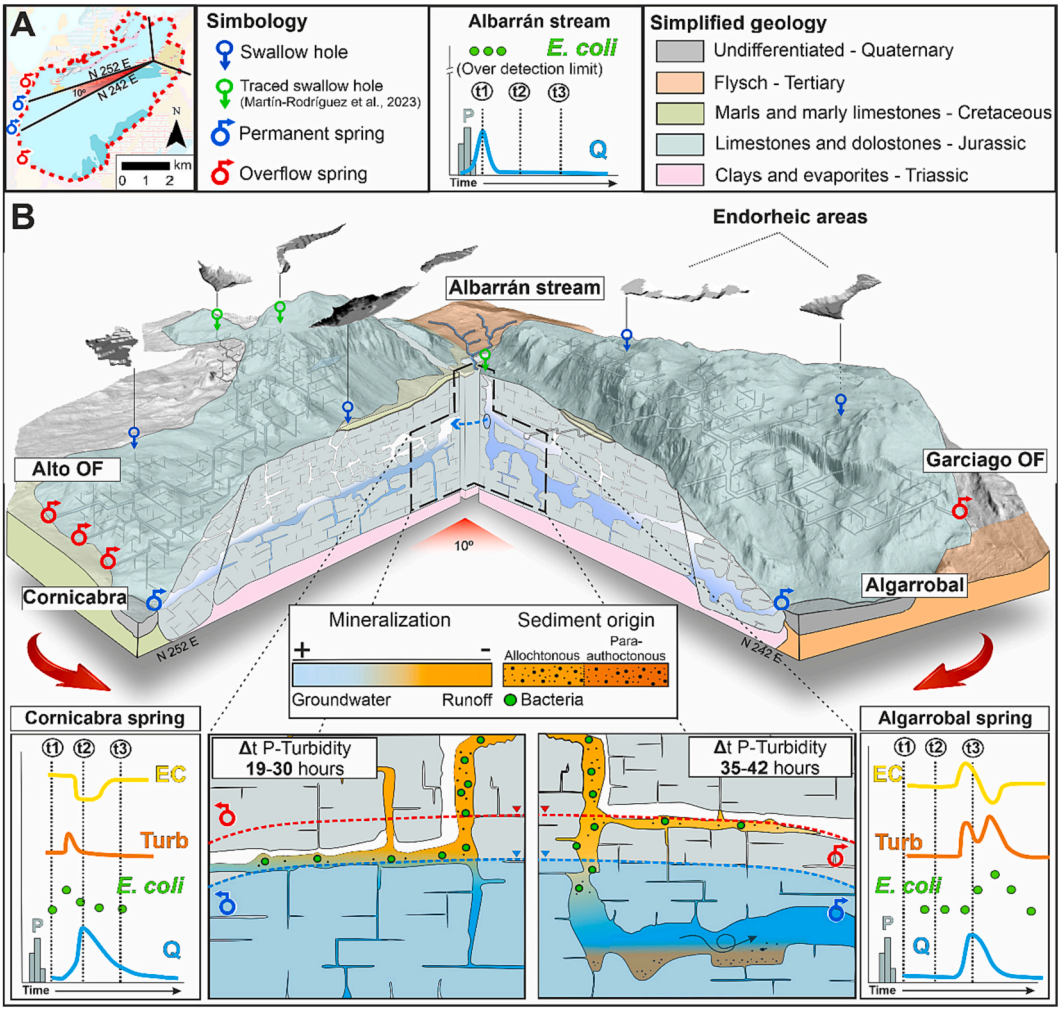

Fig. 7. A) Apparent geological sections represented in the 3D model, B) Conceptual model of Ubrique test site functioning after a recharge event in intermediate-high hydrodynamic conditions. Flow transfer from allogenic recharge to each spring and the typically produced response are represented as diagrams in the bottom part.

response of Q and TLF suggests that turbidity might come from the inner part of the system, such as the sediments stored in karst conduits and siphons. Furthermore, the usually low bacterial activity during the first turbidity peaks (Fig. 4) is coincident with abrupt increases of EC which may be related to piston-flow effect due to the drainage of the saturated zone (Fig. 7B).

This particular behaviour is similar to that described by Pronk et al. (2007) in the Jura Mountains, who described turbidity variations up to 4 NTU in absence of *E. coli* to determine the resuspension origin of para-autochthonous sediment. Mixing processes are traditionally depicted considering the evolution of EC; hence, simultaneous increases of turbidity with spring discharge and EC might indicate the mobilization of para-autochthonous sediment (e.g., Mahler et al., 1998; Massei et al., 2003; Pronk et al., 2007; Herman et al., 2008). In the same way, contemporary turbidity peaks with EC dilution intervals can be considered as a surface water flux indicator at the springs. This interpretation is coherent with the results described by several authors (e.g., Ryan and Meiman, 1996; Massei et al., 2003; Lorette et al., 2020; Goldscheider et al., 2010; Jukić and Denić-Jukić, 2023), who identified low electrical conductivity intervals in karst groundwater concomitant with turbidity maximums to assess resuspension rates of para-autochthonous sediment.

Although piston-flow effect is also observed in Cornicabra spring, the highest bacterial load is usually detected at the beginning of the flooding event (Fig. 3). This suggests a quick arrival to the spring of allogenic runoff flows from allogenic recharge through the vadose zone during the first 20–40 h after the beginning of the rain event. In addition, cross-correlation analysis highlights similar response times regarding input function for turbidity and TLF in Cornicabra spring, especially in water year 2021/2022 (Fig. 5), which suggests a similar origin of sediments and organic compounds that generate such physical responses. Subsequently, a great dilution depicted as a decrease of EC is produced due to groundwater mixing with recently infiltrated rainwater through the carbonate outcrops (Fig. 7B). Hence, the contribution from allogenic recharge in terms of water quality and sediment transport is limited to the first instants of the flooding event and then, a major contribution from diffuse recharge is manifested as low turbidity and associated bacterial activity.

Therefore, the two investigated springs display distinctive sediment transport modalities related to the local intrinsic geological features of the aquifer sector they drain (degree of functional karstification, length and morphology of conduit flow systems, etc.) and the availability of sediment sources in the spring catchment. The stated hypothesis is consistent with the results reported by Martín-Rodríguez et al. (2023) in this test site. These authors confirmed a shorter first detection time of the tracer injected in Villaluenga swallow hole in Cornicabra spring (31*h*) compared to Algarrobal (47 h), despite that the tracer recovery estimated was one order of magnitude lower in the first spring. In addition, a similar process of groundwater flow circulation to that of the Cornicabra subsystem should be produced towards the Garciago overflow spring, considering that first detection in such conditions was produced after 35 h.

5.3. New insights on early-warning strategies

5.3.1. Implementation of an operational EWS in Ubrique test site

In the case of Ubrique karst system, most of the flooding events occurred during intermediate-high flow conditions (Events 2, 3, 4, 6, 7, 8; in Figs. 3 and 4), and therefore constitute the most representative hydrogeological conditions under which contamination episodes are produced at Ubrique test site. However, the first flooding event recorded in each hydrological year (Event 1, on December 2020; and Event 5, on November 2021; in Figs. 3 and 4) after the first effective intense rainfalls presented distinctive characteristics. Prior to Event 1, minor rainfall episodes (Fig. 2) produced allogenic recharge via Villaluenga swallow hole and, therefore, the sediment input into the system. Afterwards, the more intense recharge of Event 1 mobilized the sediment accumulated during the previous months, resulting in an extremely high turbidity record at both springs. In Event 5, the highest rainfall recorded in the study period occurred, although it produced a slight hydrodynamic response (Cornicabra spring, in Fig. 3) not response at all (Algarrobal; in Fig. 4).

In addition to this exceptional behaviour of the first flooding event after long dry periods, the fact that both permanent outlets draining the same aquifer show different contamination magnitude and mixing processes after intense rain events have direct consequences in groundwater capture procedures (e.g. quick or delayed arrival of bacterial activity). Hence, the constant update of the database and statistical relationship between the investigated parameters (as stated in Fig. 8) is essential to continuously improve the EWS.

The integrated (multi-technique) approach used in this research, coupling continuous real-time record of hydroclimatic and water variables with individual bacterial analysis, constitutes a fundamental step for the development of an Early-Warning-System. The previous researches in this test site (Marín et al., 2021; Martín-Rodríguez et al., 2023) provided indispensable information for the development of the EWS (Fig. 8). Solid steps have been accomplished towards the operational implementation of an EWS in Ubrique test site. The future steps deal with online data transmission, prediction and warning dissemination for users, operators and water authorities.

5.3.2. Karst EWS and future challenges

The quick temporal variations of chemical quality and physical properties of water (such as turbidity) at some karst aquifers are well known (Ryan and Meiman, 1996) and supposes a key challenge for water companies. Early-Warning strategies adapted to karst groundwater capture have been developed in the last decade as a reliable procedure for protection of drinking water sources (Stadler et al., 2010; Storey et al., 2011; Grimmeisen et al., 2018; Guo et al., 2018; Ravbar et al., 2023). These types of techniques result from the combination of four essential elements: (1) risk knowledge, (2) monitoring, (3) prediction and warning dissemination and (4) emergency response (Grasso, 2006). The proposed scientific development of a karst groundwater contamination EWS (Fig. 8) comprises the first three elements, as the emergency response is related to technical aspects which usually depend on the water managers and local authorities.

Goldscheider et al. (2010) highlighted the importance of combining different natural tracers such as TOC or faecal bacteria with turbidity and various hydrologic and physicochemical parameters to achieve a reliable detection of microbial contamination. The approach proposed by Lorette et al. (2020) used NO_3^- and Dissolved Organic Carbon (DOC) coupled to bacterial activity to identify groundwater perturbations linked to human activities. In a recent research, Ravbar et al. (2023) highlighted the relevance of hazard and contamination risk assessment coupled to continuous monitoring for contamination early warning in karst water sources.

The results obtained in this work and in these studies highlight the importance of long-term continuous monitoring of physical responses coupled to high periodicity chemical and bacteriological analysis as the basis for risk assessment and developing a robust conceptual model of karst systems (Fig. 8). This workflow is easily transferrable to any karst aquifer with minimum adaptation according to the specificities of the system functioning and identified pressures or contaminants. Real-time monitoring and data transmission constitute as well a key aspect of EWS to rapidly detect the arrival of contamination to drinking water sources. However, few researches have analysed the potential of advanced statistical methods to improve predictions on groundwater chemical quality and remains as a future challenge for karst experts to enhance early-warning strategies.

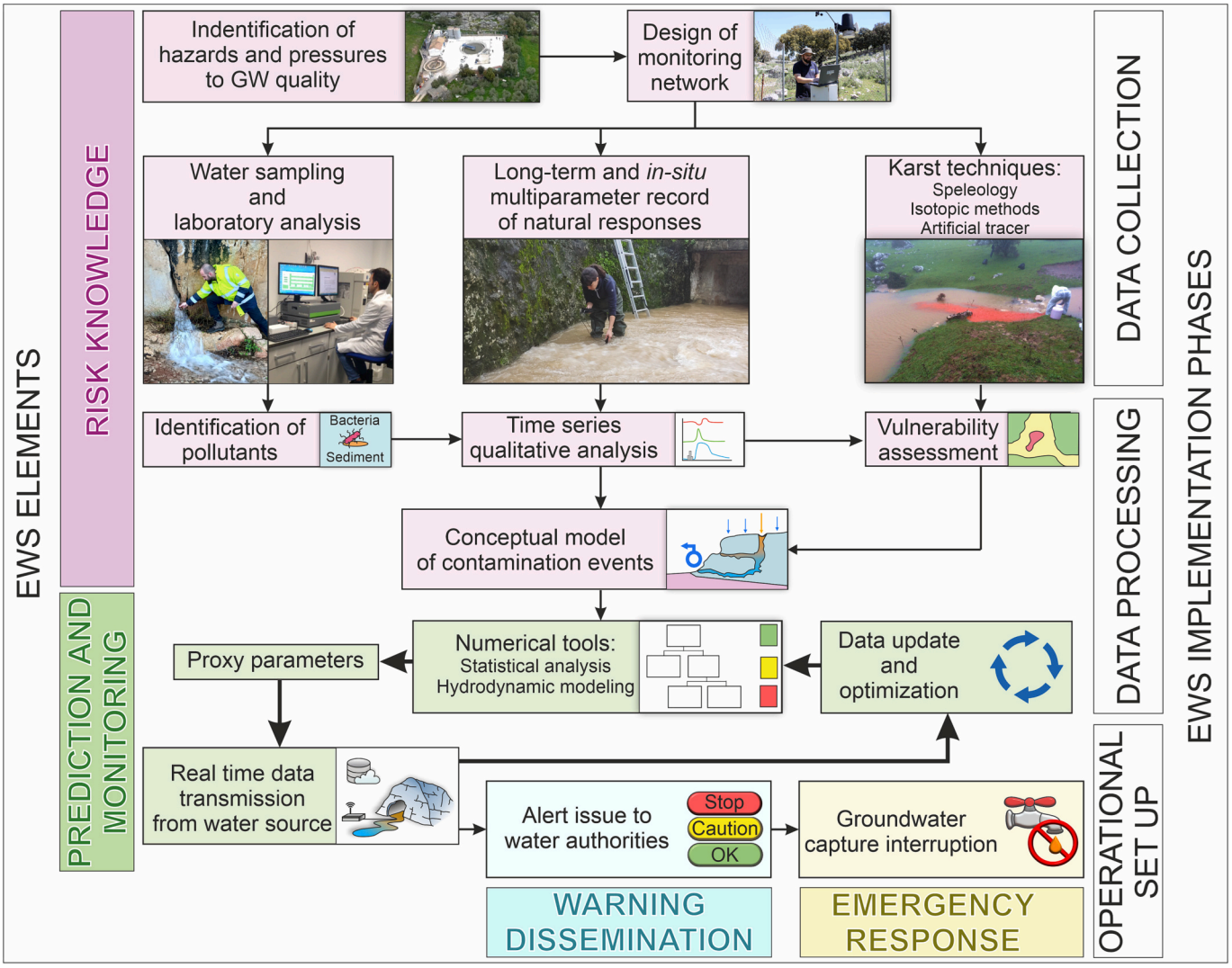

Fig. 8. Proposed scheme for the development and implementation of reliable Early-Warning-Systems (EWS) on karst groundwater with operational perspectives.

6. Conclusions

In this research, a significant progress has been achieved in the reliable development of protection strategies of karst aquifers through the detailed characterization of flooding events and temporary faecal pollution in two outlets intended for drinking water supply. The combination of karst research techniques (conventional groundwater physico-chemical parameters with microbiological analysis) was successfully applied and tested in this work to determine the main contaminant sources and to define groundwater flow modalities, sediment transport mechanisms and associated bacterial activity.

In the examined carbonate karst aquifer, located in a mountainous rural karst area in S Spain, the Wastewater Treatment Plant and the development of cattle activities in upland catchments were proved to be responsible for the high bacterial activity detected at the springs of its principal discharge zone. In spite of the natural origin of the suspended sediments, typical of binary karst systems with an important influence of allogenic recharge, it was determined that they act as the main carrier of potential pathogens. However, the differentiation between strictly allochthonous sediment and para-autochthonous sediment has important consequences in the transport of bacteria, as the mobilization of the latter type of sediment is responsible for high turbidity values in absence of bacterial activity.

The variable influence of allogenic recharge to the Sierra de Ubrique aquifer depends on the geological features of the aquifer sectors drained by each spring which determine (1) the sediment input from allogenic recharge and availability inside the system; and (2) the type of flow that control water mixing processes and sediment mobilization. Wider conduits connected to swallow holes favour the preferential circulation of allogenic recharge while siphons allow the accumulation of sediment. Such rapid flows through the vadose zone cause the mixing of para-autochthonous and allochthonous sediment with bacterial load, while piston-type flows cause the mobilization of the para-autochthonous sediment from siphons in first place.

Due to the high heterogeneity and vulnerability to contamination of karst media, the continuous monitoring of hydroclimatic variables and individual spring response coupled to individual bacteria analysis constitutes a suitable tool to develop a conceptual model to unravel pollutant transfer processes in groundwater. The analysis of bacterial activity coupled to traditional methods in karst hydrogeology is essential for an adequate protection of water sources for drinking use. This study sets the basis for a further development of Early-Warning strategies, considering online parameters (rainfall, spring discharge, EC, temperature, turbidity and Tryptophan-Like-Fluorescence) for prevention of public health issues. The proposed methodology to design a reliable EWS is easily transferrable to any kind of karst aquifer with slight adaptations according to the identified pressures and system functioning.

CRediT authorship contribution statement

Jaime Fernández-Ortega: Conceptualization, Data curation, Formal analysis, Investigation, Methodology, Writing – original draft, Writing – review & editing. **Juan Antonio Barberá:** Conceptualization, Methodology, Project administration, Writing – review & editing. **Bartolomé Andreo:** Conceptualization, Methodology, Funding acquisition, Project administration, Writing – review & editing.

Declaration of competing interest

The authors declare that they have no competing financial or personal interests that could have influenced the work presented in this paper.

Data availability

Data will be made available on request.

Acknowledgements

This research is a contribution to the PRIMA funded European project KARMA (Karst Aquifer Resources availability and quality in the Mediterranean Area – ANR-18-PRIM-0005); the Spanish project (ref. PCI2019-103675) funded by the International Joint Programme of the Ministry of Science, Innovation and Universities; the project PID2019-111759RB-I00; and to the Research Group RNM-308 of the Junta de Andalucía, funded by the Autonomous Government of Andalusia (Spain). The authors thank the local government of Ubrique town and the local water company "Empresa Mixta de Aguas de Ubrique" and the authorities of the Sierra de Grazalema Natural Park for its collaborative behaviour. Funding for open access charge: Universidad de Málaga / CBUA.

References

Allocca, V., Celico, F., Petrella, E., Marzullo, G., Naclerio, G., 2008. The role of land use and environmental factors on microbial pollution of mountainous limestone aquifers. Environ. Geol. 55, 277–283. https://doi.org/10.1007/s00254-007-1002-5.

Auckenthaler, A., Raso, G., Huggenberger, P., 2002. Particle transport in a karst aquifer: natural and artificial tracer experiments with bacteria, bacteriophages and microspheres. Water Sci. Technol. 46 (3), 131–138. https://doi.org/10.2166/wst.2002.0072.

Beaudeau, P., Le, T.A., Zeghnoun, A., Zanobetti, A., Schwartz, J., 2012. A time series study of drug sales and turbidity of tap water in Le Havre, France. J. Water Health 10 (2), 221–235. https://doi.org/10.2166/wh.2012.157.

Bicalho, C.C., Batiot-Guilhe, C., Seidel, J.L., Van Exter, S., Jourde, H., 2012. Hydrodynamical changes and their consequences on groundwater hydrochemistry induced by three decades of intense exploitation in a Mediterranean karst system. Environ. Earth Sci. 65 (8), 2311–2319. https://doi.org/10.1016/j.jhydrol.2012.04.059.

Boyer, D.G., Pasquarell, G.C., 1999. Agricultural land use impacts on bacterial water quality in a karst groundwater aquifer. J. Am. Water Resour. Assoc. 35 (2), 291–300. https://doi.org/10.1111/j.1752-1688.1999.tb03590.x.

Buckerfield, S.J., Quilliam, R.S., Bussiere, L., Waldron, S., Naylor, L.A., Li, S., Oliver, D. M., 2020. Chronic urban hotspots and agricultural drainage drive microbial pollution of karst water resources in rural developing regions. Sci. Total Environ. 744. https://doi.org/10.1016/j.scitotenv.2020.140898.

Chen, Z., Auler, A.S., Bakalowicz, M., Drew, D., Griger, F., Hartmann, J., Jiang, G., Moosdorf, N., Richts, A., Stevanovic, Z., Veni, G., Goldscheider, N., 2017. The world karst aquifer mapping project: concept, mapping procedure and map of Europe. Hydrogeol. J. 25, 771–785. https://doi.org/10.1007/s10040-016-1519-3.

Cuk Đurovic, M., Petric, M., Jemcov, I., Mulec, J., Grudnik, Z.M., Mayaud, C., Blatnik, M., Kogovšek, B., Ravbar, N., 2022. Multivariate statistical analysis of hydrochemical and microbiological natural tracers as a tool for understanding karst hydrodynamics (the Unica Springs, SW Slovenia). Water Resour. Res. 58 https://doi.org/10.1029/2021WR031831.

Karst hydrogeology and human activities: impacts, consequences and implications. In: Drew, D., Hötzl, H. (Eds.), 1999. International Contributions to Hydrogeology, 20. Balkema, Rotterdam, The Netherlands, 338 pp.

Einsiedl, F., Mayer, B., 2006. Hydrodynamic and microbial processes controlling nitrate in a fissured-porous karst aquifer of the Franconian Alb, Southern Germany. Environ. Sci. Technol. 40, 6697–6702. https://doi.org/10.1021/es061129x.

Epting, J., Page, R.M., Auckenthaler, A., Huggenberger, P., 2018. Process-based monitoring and modeling of karst springs e linking intrinsic to specific vulnerability. Sci. Total Environ. 625, 403–415. https://doi.org/10.1016/j.scitotenv.2017.12.272.

Foster, S., Hirata, R., Gomes, D., D'Elia, M., Paris, M., 2002. Groundwater Quality Protection. https://doi.org/10.1596/0-8213-4951-1.

Frank, S., Fahrmeier, N., Goeppert, N., Goldscheider, N., 2022. High-resolution multi-parameter monitoring of microbial water quality and particles at two alpine karst springs as a basis for an early-warning system. Hydrogeol. J. 30, 2285–2298. https://doi.org/10.1007/s10040-022-02556-8.

Geiger, R., 1954. Klassifikation der Klimate nach W. Köppen [Classification of climates after W. Köppen]. Landolt-Börnstein–Zahlenwerte und Funktionen aus Physik, Chemie, Astronomie, Geophysik und Technik, alte Serie, 3. Springer, Berlin, pp. 603–607.

Goldscheider, N., 2005. Karst groundwater vulnerability mapping: application of a new method in the Swabian Alb, Germany. Hydrogeol. J. 13 (4), 555–564. https://doi.org/10.1007/s10040-003-0291-3.

Goldscheider, N., Drew, D., 2007. Methods in karst hydrogeology. Taylor & Francis, London.

Goldscheider, N., Pronk, M., Zopfi, J., 2010. New insights into the transport of sediments and microorganisms in karst groundwater by continuous monitoring particle size distribution. Geol. Croat. 63, 137–142. https://doi.org/10.4154/gc.2010.10.

Grasso, V.F., 2006. Seismic Early Warning Systems: Procedure for automated decision making, University of Naples "Federico II", Ph.D. thesis. http://www.fedoa.unina.it/825/.

Grimmeisen, F., Riepl, D., Schmidt, S., Xanke, J., Goldscheider, N., 2018. Set-up of an early warning system for an improved raw water management of karst groundwater resources in the semi-arid side Wadis of the Jordan Valley. In: Geophysical Research Abstracts, 20. EGU2018-16731, EGU General Assembly.

Guo, Y., Wu, Q., Li, C., Zhao, Z., Sun, B., He, S., Jiang, G., Zhai, Y., Guo, F., 2018. Application of the risk-based early warning method in a fracture-karst water source, North China. Water Environ. Res. 90 (3), 206–219. https://doi.org/10.2175/106143017X15131012152771.

Hagedorn, C., 1984. Microbial aspects of groundwater pollution due to septic tanks. In: Bitton, G., Gerba, C.P. (Eds.), Groundwater Pollution Microbiology. Wiley, New York, pp. 181–195.

Heinz, B., Birk, S., Liedl, R., Geyer, T., Straub, K.L., Andresen, J., Bester, K., Kappler, A., 2009. Water quality deterioration at a karst spring (Gallusquelle, Germany) due to combined sewer overflow: evidence of bacterial and micro-pollutant contamination. Environ. Geol. 57 (4), 797–808. https://doi.org/10.1007/s00254-008-1359-0.

Herman, E.K., Toran, L., White, W.B., 2008. Threshold events in spring discharge: evidence from sediment and continuous water level measurement. J. Hydrol. 351, 98–106. https://doi.org/10.1016/j.jhydrol.2007.12.001.

Herman, E.K., Toran, L., White, W.B., 2012. Clastic sediment transport and storage in fluviokarst aquifers: an essential component of karst hydrogeology. Carbonates Evaporites 27, 211–241. https://doi.org/10.1007/s13146-012-0112-7.

IGME, 1984. Estudio de investigación hidrogeológica para la regulación de recursos hídricos en la divisoria Guadalete-Guadiaro. Cádiz-Málaga.

Jukić, D., Denić-Jukić, V., 2023. An alternative approach to investigation of sediment transport through a karst aquifer. J. Hydrol. 625, 130037 https://doi.org/10.1016/j.jhydrol.2023.130037.

Junta de Andalucía, 2021. Plan Hidrológico de la Cuenca Guadalete-Barbate: Ciclo 2022–2027. Esquema de temas importantes, Anexo I.

Kresic, N., Stevanovic, Z., 2010. Groundwater Hydrology of Springs. Management, and Sustainability. Elsevier. Engineering Theory. p 592p.

Li, S.L., Liu, C.Q., Lang, Y.C., Zhao, Z.Q., Zhou, Z.H., 2010. Tracing the sources of nitrate in karstic groundwater in Zunyi, Southwest China: a combined nitrogen isotope and water chemistry approach. Environ. Earth Sci. 60, 1415–1423. https://doi.org/10.1007/s12665-009-0277-0.

Lorette, G., Peyraube, N., Lastennet, R., Denis, A., Sabidussi, J., Fournier, M., Viennet, D., Gonand, J., Villanueva, J.D., 2020. Tracing water perturbation using NO3−, doc, particles size determination, and bacteria: a method development for karst aquifer water quality hazard assessment. Sci. Total Environ. 725, 138512. ISSN 0048-9697. https://doi.org/10.1016/j.scitotenv.2020.138512.

Mahler, B.J., Lynch, F.L., 1999. Muddy waters: temporal variation in sediment discharging from a karst spring. J. Hydrol. 214 (1–4), 165–178. https://doi.org/10.1016/S0022-1694(98)00287-X.

Mahler, B.J., Bennett, P.C., Zimmerman, M., 1998. Lanthanide-labeled clay: a new method for tracing sediment transport in karst. Ground Water 36, 835–843.

Mahler, B.J., Personne, J.C., Lods, G.F., Drogue, C., 2000. Transport of free and particulate-associated bacteria in karst. J. Hydrol. 238 (3–4), 179–193. https://doi.org/10.1016/S0022-1694(00)00324-3.

Marín, A.I., Martín Rodríguez, J.F., Barberá, J.A., Fernández-Ortega, J., Mudarra, M., Sánchez, D., Andreo, B., 2021. Groundwater vulnerability to pollution in karst aquifers, considering key challenges and considerations: application to the Ubrique springs in southern Spain. Hydrogeol. J. 29, 379–396. https://doi.org/10.1007/s10040-020-02279-8.

Martín-Algarra, M., 1987. Evolución geológica alpina del contacto entre las Zonas Internas y Externas de la Cordillera Bética. PhD Thesis. University of Granada, Spain, 1171 pp.

Martín-Rodriguez, J.F., Mudarra, M., Andreo, B., Sánchez, D., 2019. Analysis of the Water Turbidity in Karst Springs From S Spain and Its Relationship With Other Natural Responses, Contribution ID: 712, Poster at 46th IAH Congress. Malaga, Spain, p. 2019. September.

Martín-Rodríguez, J.F., Mudarra, M., De la Torre, B., Andreo, B., 2023. Towards a better understanding of time-lags in karst aquifers by combining hydrological analysis tools

and dye tracer tests. Application to a binary karst aquifer in southern Spain. J. Hydrol. 621, 129643 https://doi.org/10.1016/j.jhydrol.2023.129643.
Massei, N., Wang, H.Q., Dupont, J.P., Rodet, J., Laignel, B., 2003. Assessment of direct transfer and resuspension of particles during turbid floods at a karstic spring. J. Hydrol. 275 (1–2), 109–121. https://doi.org/10.1016/S0022-1694(03)00020-9.
Mendoza, D., 1992. La Sima de Villaluenga. Historia del primer descenso, 6. Boletín del Museo Andaluz de la Espeleología, Granada, pp. 3–8.
Musgrove, M., Opsahl, S.P., Mahler, B.J., Herrington, C., Sample, T.L., Banta, J.R., 2016. Source, variability, and transformation of nitrate in a regional karst aquifer: Edwards aquifer, central Texas. Sci. Total Environ. 568, 457–469. https://doi.org/10.1016/j.scitotenv.2016.05.201.
Nilsson, L., Widerlund, A., 2017. Tracing nitrogen cycling in mining waters using stable nitrogen isotope analysis. Appl. Geochem. 84, 41–51. https://doi.org/10.1016/j.apgeochem.2017.05.025.
Olstadt, J., Schauer, J.J., Standridge, J., Kluender, S., 2007. A comparison of ten USEPA approved total coliform/E. coli tests. J. Water Health 5, 267–282. https://doi.org/10.2166/wh.2007.008b.
Padilla, A., Pulido-Bosch, A., 1995. Study of hydrographs of karstic aquifers by means of correlation and cross-spectral analysis. J. Hydrol. 168, 73–89. https://doi.org/10.1016/0022-1694(94)02648-U.
Palmateer, G., McLean, D., Kutas, W., Meissner, S., 1993. Suspended particulate/bacterial interaction in agricultural drains. In: Rao, S.S. (Ed.), Particulate Matter and Aquatic Contaminants, Lewis Publishers. Fl, Boca Raton.
Pommepuy, M., Guillaud, J.F., Dupray, E., Derrien, A., Le Guyader, F., Cormier, M., 1992. Enteric bacteria survival factors. Water Sci. Technol. 25, 93–103.
Pronk, M., Goldscheider, N., Zopfi, J., 2007. Particle-size distribution as indicator for faecal bacteria contamination of drinking water from karst springs. Environ. Sci. Technol. 41 (24), 8400–8405. https://doi.org/10.1021/es071976f.
R Core Team, 2021. R: A Language and Environment for Statistical Computing. R Foundation for Statistical Computing, Vienna, Austria. https://www.R-project.org/.
Ravbar, N., Mulec, J., Mayaud, C., Blatnik, M., Kogovšek, B., Petrič, M., 2023. A comprehensive early warning system for karst water sources contamination risk, case study of the Unica springs, SW Slovenia. Sci. Total Environ. 885, 163958 https://doi.org/10.1016/j.scitotenv.2023.163958.
RD 3/2023, 2023. Real Decreto-ley de 10 de enero, por el que se establecen los criterios técnico-sanitarios de la calidad del agua de consumo, su control y suministro. Boletín Oficial del Estado, pp. 4253–4354 núm. 9, de 11 de enero de. (102 págs.).
Reed, S.C., Middlebrooks, E.J., Crites, R.W., 1988. In: Reed, S.C., Sherwood, S. (Eds.), Natural Systems for Waste Management and Treatment. McGraw-Hill, New York.
Ryan, M., Meiman, J., 1996. An examination of short-term variations in water quality at a karst spring in Kentucky. Ground Water 34 (1), 23–30. https://doi.org/10.1111/j.1745-6584.1996.tb01861.x.
Sánchez, D., Barberá, J.A., Mudarra, M., Andreo, B., Martín, J.F., 2018. Hydrochemical and isotopic characterization of carbonate aquifers under natural flow conditions, Sierra Grazalema Natural Park, southern Spain. In: Parise, M., Gabrovsek, F., Kaufmann, G., Ravbar, N. (Eds.), Advances in Karst Research: Theory, Fieldwork and Applications, 466. Geol Soc London Spec Publ, pp. 275–293. https://doi.org/10.1144/SP466.16.
Sorensen, J.P.R., Lapworth, D.J., Marchant, B.P., Nkhuwa, D.C.W., Pedley, S., Stuart, M. E., Bell, R.A., Chirwa, M., Kabika, J., Liemisa, M., Chibesa, M., 2015. In situ tryptophan-like fluorescence: a real-time indicator of faecal contamination in drinking water supplies. Water Res. 81, 38–46. https://doi.org/10.1016/j.watres.2015.05.035.
Stadler, H., Klock, E., Skritek, P., Mach, R.L., Zerobin, W., Farnleitner, A.H., 2010. The spectral absorption coefficient at 254 nm as a real-time early warning proxy for detecting faecal pollution events at alpine karst water resources. Water Sci. Technol. 62 (8), 1898–1906. https://doi.org/10.2166/wst.2010.500.
Stevanović, Z., 2019. Karst waters in potable water supply: a global scale overview. Environ. Earth Sci. 78, 662. https://doi.org/10.1007/s12665-019-8670-9.
Storey, M.V., van der Gaag, B., Burns, B.P., 2011. Advances in on-line drinking water quality monitoring and early warning systems. Water Res. 45 (2), 0–747. https://doi.org/10.1016/j.watres.2010.08.049.
USEPA, 1986. Septic Systems and Groundwater Protection: An Executive Guide. U.S. Environmental Protection Agency, Office of Groundwater Protection, Washington, DC.
White, W.B., 1988. Geomorphology and Hydrology of Karst Terrains. Oxford University Press, New York, p. 464.
Yang, P.H., Li, Y., Groves, C., Hong, A., 2019. Coupled hydrogeochemical evaluation of a vulnerable karst aquifer impacted by septic effluent in a protected natural area. Sci. Total Environ. 658, 1475–1484. https://doi.org/10.1016/j.scitotenv.2018.12.172.
Yang, P.H., Wang, Y.Y., Wu, X.Y., Chang, L.R., Ham, B., Song, L.S., Groves, C., 2020. Nitrate sources and biogeo-chemical processes in karst underground rivers impacted by different anthropogenic input characteristics. Environ. Pollut. 265, 114835 https://doi.org/10.1016/j.envpol.2020.114835.
Zar, J.H., 2008. Spearman Rank Correlation Coefficient. Springer, New York, pp. 502–505. https://doi.org/10.1007/978-0-387-32833-1 379.
Zobell, C.E., 1943. The effect of solid surfaces on bacterial activity. J. Bacteriol. 46, 39–56.